

LA-10232-SR
Status Report

UC-33A
Issued: December 1984

LA--10232-SR

DE85 007392

General-Purpose Heat Source Development: Safety Test Program

Postimpact Evaluation, Design Iteration Test 5

T. G. George
F. W. Schonfeld

DISCLAIMER

This report was prepared as an account of work sponsored by an agency of the United States Government. Neither the United States Government nor any agency thereof, nor any of their employees, makes any warranty, express or implied, or assumes any legal liability or responsibility for the accuracy, completeness, or usefulness of any information, apparatus, product, or process disclosed, or represents that its use would not infringe privately owned rights. Reference herein to any specific commercial product, process, or service by trade name, trademark, manufacturer, or otherwise does not necessarily constitute or imply its endorsement, recommendation, or favoring by the United States Government or any agency thereof. The views and opinions of authors expressed herein do not necessarily state or reflect those of the United States Government or any agency thereof.

MASTER

DISTRIBUTION OF THIS DOCUMENT IS UNLIMITED

Los Alamos Los Alamos National Laboratory
Los Alamos, New Mexico 87545

GENERAL-PURPOSE HEAT SOURCE DEVELOPMENT: SAFETY TEST PROGRAM

Postimpact Evaluation, Design Iteration Test 5

by

T. G. George and F. W. Schonfeld

ABSTRACT

The General-Purpose Heat Source (GPHS) provides power for space missions by transmitting the heat of ^{238}Pu decay to thermoelectric elements. Because of the inevitable return of certain aborted missions, the heat source must be designed and constructed to survive both re-entry and Earth impact. The Design Iteration Test (DIT) series is part of an ongoing impact test program. The fifth test (DIT-5) was designed to compare the impact response of a GPHS fueled clad that had been welded with a four-pole arc oscillator with the impact response of a clad welded with a two-pole oscillator. In DIT-5 a partial GPHS module containing two fueled clads (one welded with a four-pole oscillator and one welded with a two-pole oscillator) was impacted at 60.5 m/s and 930°C. The fuel capsules were severely deformed by the impact; both clads breached. The capsule welded with a four-pole oscillator failed extensively. Neither failure was related to the welding technique. Postimpact analyses of the test components are described, with emphasis on microstructure and impact response.

I. INTRODUCTION

The General-Purpose Heat Source (GPHS) is a modular component of the radioisotope thermoelectric generator (RTG) that will provide power for a number of space missions. The first two uses will be the 1986 NASA Galileo and Ulysses (formerly ISPM) missions. The RTG generates electricity by using the heat of ^{238}Pu alpha decay to create a temperature differential across a thermoelectric array; each GPHS module provides a total thermal output of 250 W. The RTG contains eighteen GPHS modules, each with four $^{238}\text{PuO}_2$ fuel pellets encapsulated in DOP-26 iridium clads. The Galileo mission will require two RTGs, and the Ulysses mission will use a single RTG.

In addition to the inevitable return of near-Earth missions, the probability of a launch abort can never be zero. Therefore, the GPHS module must be designed

and constructed to survive both re-entry and Earth impact. The results described in this report are a portion of an ongoing test program and will provide necessary design and safety analysis information.

Previous Design Iteration Tests evaluated impact responses with changes in module orientation,^{1,2} changes in the fueled clad processing,^{3,4} and internal weld defects.² DIT-5 was included in the test series to compare the impact response of a fueled clad welded with a four-pole arc oscillator with the response of a clad welded with a two-pole oscillator. In the test, two fueled clads supplied by the Savannah River Plant (SRP) [designated SRP-423 (two-pole weld) and SRP-444 (four-pole weld)] were loaded into a partial aeroshell and impacted at 60.5 m/s and 930°C. The primary objective of the test was to compare the quality and survivability of the welds; this report emphasizes the weld structures and their performance.

H. PRETEST DATA

The iridium cups and fuel pellets used in the assembly of the DIT-5 heat sources are identified in Table I; data describing the fuel pellets are presented in Table II. As in previous DIT tests, SRP produced the fuel pellets and did the capsule assembly and welding, Oak Ridge National Laboratory (ORNL) provided the iridium alloy blanks and produced the graphite insulation [carbon-bonded carbon filament (CBCF)], the Mound Facility (MF) fabricated the iridium cups, and Los Alamos machined the aeroshell and impact shells from Fineweave-Pierced Fabric* (FWPF) graphite.

Each DIT-5 fueled clad was macroscopically examined for external weld defects. Both clads had good wall alignment over the entire weld length. The weld overlaps were uniform and contained no obvious defects; no bulges or other anomalies were observed in either capsule.

After macroscopic examination, the fueled clads were radiographed and loaded into a graphite impact shell (GIS). The GIS was then aged at 1310°C for 30 days (a heat treatment designed to simulate the minimum expected service life). Following heat treatment, the fuel capsules were radiographed again. The pre- and post-aging radiographs (Figs. 1 and 2) indicate that both fuel pellets were severely cracked and that the aging treatment did not markedly increase the fuel breakup.

III. TEST PROCEDURE

After post-aging radiography, the fueled GIS was loaded into a partial GPHS module as shown in Fig. 3. Fueled clad SRP-423 was located in the blind end of the impact shell and SRP-444 was at the closure end (the SRP fuel labels are used throughout this report to identify the fuel/clad sets). The test module was impacted "flat on" (against the broad aeroshell face containing the flight control surfaces) at 60.5 m/s and 930°C. After the test, a sealed catch tube containing the impacted module was transferred to Wing 2 of the CMR Building (at Los Alamos) and was opened in a hood. The postimpact procedures used in DIT-5 were the same as those applied in previous Design Iteration Tests.

IV. POSTIMPACT EXAMINATION

Experience with previous Design Iteration Tests expedited postimpact disassembly. The catch tube was

*Fineweave-Pierced Fabric 3-D carbon/carbon composite, a product of AVCO Systems Division, 201 Lowell St., Wilmington, MA 01887.

TABLE I. Encapsulation Details for the DIT-5 Capsules

Capsule	Iridium Cup		Fuel Pellet
	Vent	Blind	
SRP-423	S26-4	S26-5	8206HF423
SRP-444	S13-5	S9-6	8207HF444

placed in an open-fronted hood and the pump-out plug was removed. A swab inserted into the pump-out hole registered $>50\,000$ counts/min/cm²; the elevated swipe count indicated the extensive failure of one or both clads. The end of the catch tube was carefully removed, and the inner nickel can (a thermal radiation shield containing the half module) was extracted and placed on a bed of solid CO₂. The CO₂ cooled the assembly rapidly, and in a few minutes, the temperature had dropped far enough to prevent combustion of the graphite.

Aeroshell damage was moderate (Fig. 4). A corner of the aeroshell had broken off, and the aeroshell cap had been removed, but the GIS remained in place. The impact shell sustained significant damage (Fig. 5). The GIS cap was partially removed, and numerous longitudinal cracks extended the length of the impact face (Fig. 5a). The trailing face of the GIS contained several short longitudinal cracks and a long horizontal crack that appeared to follow the closure threads (Fig. 5c). The GIS exhibited the same bowed profile (Fig. 5b) observed in impact shells used in previous DIT tests.

The fuel capsules were extracted from the remains of the impact shell, macroscopically examined, photographed, and measured. Side and end views of each capsule are shown in Fig. 6. Capsule SRP-423 was breached by a narrow crack (approximately 0.1×10.0 mm) on the impact face of the vent cup (Fig. 7). SRP-444 was severely cracked on the impact face: a wide longitudinal crack (~ 2.0 mm wide) extended the length of the capsule and into the cup radii (Fig. 8). A second crack (0.2×10.0 mm), parallel to the main fracture, was observed on the SRP-444 vent cup.

Although both DIT-5 clads breached, the capsule deformations were consistent with the deformations observed in previous DIT impacts. Capsule dimensions and calculated gross strains are listed in Tables III and IV.

TABLE II. Data for the DIT-5 Fuel Pellets

Pellet	Diameter (mm)	Length (mm)	Weight (g)
HF-423	27.44	27.57	150.2
HF-444	nonintegral at loading		151.1

TABLE III. Dimensions of DIT-5 Fueled Clads

Preimpact Dimensions (mm)		Clad Numbers	
		SRP-423	SRP-444
Diameter			
Vent Cup		29.82	29.85
Weld		29.92	29.90
Blind Cup		29.79	29.79
Length		30.05	30.07
Diagonal		37.45	37.47
Postimpact Dimensions (mm)		Clad Numbers	
		SRP-423	SRP-444
Diameter			
Vent Cup	min	27.38	26.59
	max	32.36	33.02
Weld	min	27.41	26.92
	max	33.02	33.58
Blind Cup	min	27.00	26.97
	max	32.33	32.64
Length	min	30.35	30.35
	max	31.95	31.75
Diagonal	min	36.07	35.56
	max	38.35	38.71

TABLE IV. DIT-5 Postimpact Capsule Strains

		Clad Numbers	
		SRP-423	SRP-444
Diameter			
Vent Cup	min	- 8.2%	- 10.9%
	max	+ 8.5	+10.6
Weld	min	- 8.5	- 9.9
	max	+10.3	+12.3
Blind Cup	min	- 9.4	- 9.5
	max	+ 8.5	+ 9.6
Length	min	+ 1.0	+ 0.9
	max	+ 6.3	+ 5.6
Diagonal	min	- 3.7	- 5.1
	max	+ 2.4	+ 3.3

V. CAPSULE OPENING AND FUEL SAMPLING

An abrasive cutting wheel was used to make a small circumferential slit 6-8 mm above the weld (vent cup) on each capsule. Contact between the abrasive wheel and the fuel pellet was reduced by minimizing breakthrough of the capsule wall. The remaining capsule wall on SRP-444 was pried open with a small screwdriver; the clad was defueled immediately after it was opened. For determination of the quantity of respirable fuel particles produced by impact, capsule SRP-423 was transferred to a glovebox train used for fines analysis and opened underwater to avoid the loss of small fuel fragments.

The opened capsules were examined with a hand-held magnifier. No fractures (other than the breaching cracks previously described) or other defects were visible on the capsule exteriors. Examination of the clad interiors revealed numerous small cracks in the capsule walls and closure welds. All cracked areas were removed for metallographic examination.

A face-on weld sample was obtained from each capsule in accordance with SRP procedure DPSOL 235-F-PuFF-3129M.⁵ The weld in each capsule was also sampled to provide specimens from the overlap and single-pass regions. The weld samples included wall sections large enough to establish grain size, other microstructural features, and hardness of the weld-shield cup. Similarly, the vent cup sections established grain size and revealed other microstructural features. Samples of the two cups making up each capsule were submitted for spectrographic and Auger electron spectroscopic analyses. The spectrographic samples were cut from the capsule walls at about mid-height.

The fuel extracted from SRP-444 was sampled for ceramography by the selection of two 1-g fragments: one fragment from the outer edge of the pellet and one fragment from the pellet center. Two additional 1-g fragments were removed for chemical analysis: one for spectrographic analysis and one for a wet-chemistry phosphorus determination. The fuel in capsule SRP-423 was not sampled until after the particle-size analysis had been completed; results of the sieve analysis are presented in Tables V and VI. After the remains of each fuel pellet had been repackaged for transfer, each lot was radioanalyzed to approximate the phosphorus content.

VI. METALLOGRAPHIC EXAMINATION

A. Weld Metallography

After the DIT-5 capsules had been opened and defueled, the interior weld surfaces were macroscopically

TABLE V. Sieve Analysis of the Fuel Remaining in Capsule SRP-423

Particle Size (μm)	Weight Fraction	Accumulated
		Weight Fraction
+6000	0.2774	0.2774
+2000	0.3958	0.6733
+ 841	0.2030	0.8763
+ 420	0.0626	0.9388
+ 177	0.0291	0.9679
+ 125	0.0050	0.9730
+ 74	0.0056	0.9786
+ 44	0.0058	0.9844
+ 30	0.0048	0.9892
+ 20	0.0046	0.9938
+ 10	0.0040	0.9977
- 10	0.0023	1.0000

examined for weld defects. All cracked areas were removed for metallographic examination. In addition, each weld was sampled to provide overlap, single-pass, and face-on specimens in accordance with SRP procedure DPSOL 235-F-PuFF-3129M. Results of the metallographic examinations are given below.

1. SRP-423 (two-pole arc oscillator). The internal surface of the overlap weld is shown in Fig. 9; two small cracks are visible just beyond the weld submergence. Deep weld cracks were observed in a reverse bend on the impact face (Fig. 10). Although the large crack was recognized as a portion of the breach, metallographic examination revealed that one of the other cracks also penetrated the capsule wall (Fig. 11). The single-pass weld specimen (Fig. 12) did not contain any cracks and

TABLE VI. Subsieve Particle Distribution of SRP-423 Fuel

Particle Size Range (μm)	Number of Particles	Weight Fraction	Accumulated
			Weight Fraction
0 to 1	2030	0.000241	0.000241
1 to 2	125	0.000119	0.000360
2 to 3	42	0.000135	0.000495
3 to 4	6	0.000046	0.000540
4 to 5	8	0.000119	0.000659
5 to 6	7	0.000180	0.000839
6 to 7	11	0.000448	0.001287
7 to 8	5	0.000304	0.001591
8 to 9	2	0.000173	0.001765
9 to 10	4	0.000475	0.002240

was essentially free of porosity. The overlap specimen, however, contained a significant amount of porosity and had a somewhat coarse microstructure (Fig. 13). The face-on weld specimen was typical (Fig. 14).

2. SRP-444 (four-pole arc oscillator). Examination of the clad interior revealed a long section of incomplete weld penetration; the cup edges were clearly visible over a 120° arc of closure weld. In addition, numerous transverse weld cracks were observed in a reverse bend on the impact face (Fig. 15). All of the cracks were intergranular (Fig. 16), and the deepest crack penetrated more than 50% of the capsule wall. The section of closure weld containing the point of weld submergence was free of defects (Fig. 17). Microscopic examination of the overlap weld revealed an unusual amount of porosity (Fig. 18a) and an otherwise typical microstructure (Fig. 18b). Examination of single-pass weld specimens from regions of complete (Fig. 19) and incomplete (Fig. 20) weld penetration revealed only slight microstructural differences. The microstructure of the face-on weld specimen (Fig. 21) was acceptable.

B. Iridium-Cup Wall Microstructure

Macroscopic examination of the capsule interiors did not reveal any surface defects other than the breaching and weld cracks described previously. Each capsule was sampled to provide specimens for metallography; the cup portions removed included severely deformed wall sections, undisturbed wall sections, and cross sections of the breaching cracks. The results of microhardness tests conducted on the cup samples are presented in Table VII. The cup grain sizes are listed in Table VIII. Results of the metallographic examinations are summarized below.

TABLE VII. Postimpact Hardness of the DIT-5 Capsules

Capsule	Location	DPHN (2000-g load)	
		@95% CL ^a	Range
SRP-423	Vent Cup	310 ± 4	302 - 326
	Weld	323 ± 11	291 - 347
	Blind Cup	321 ± 11	298 - 348
SRP-444	Vent Cup	334 ± 6	313 - 347
	Weld	337 ± 13	310 - 364
	Blind Cup	328 ± 8	310 - 355

^aCL = confidence level.

TABLE VIII. Grain Size in the DIT-5 Capsules

Capsule	Grains/ Thickness*
SRP-423	
Vent Cup	17.9
Blind Cup	15.5
SRP-444	
Vent Cup	19.6
Blind Cup	18.7

*Average number of grains/0.635-mm nominal wall thickness.

1. **SRP-423 (two-pole arc oscillator).** Examination of a vent cup section containing the breaching crack (Fig. 22) revealed the same intergranular crack morphology observed in previous clad failures. Although wall material adjacent to the breach was relatively fine grained (~16 grains/0.635-mm wall thickness), there was little evidence of plastic deformation. Interestingly, vent cup sections removed from reverse bends near the breaching crack demonstrated a surprising amount of ductility (Figs. 23 and 24). The wall material in a sharp bend only 4 mm from the breach (Fig. 23) was particularly ductile, displaying a significant amount of grain elongation.

Examination of a transverse section removed from the SRP-423 vent cup revealed a large pore (Fig. 25) with an apparent diameter equivalent to 25% of the total wall thickness. The pore was located nearly 3 mm from the weld centerline and would not be expected to have been within the fusion or heat-affected zones.

The iridium grain size in the SRP-423 cups ranged from 15 to 22 grains/0.635-mm nominal wall thickness. Although isolated areas of grain growth were observed in the vent cup (Fig. 26), the microstructure was generally fine grained (Fig. 27). The shield cup also had a fine-grained microstructure (Fig. 28).

2. **SRP-444 (four-pole arc oscillator).** Examination of a shield cup section containing the main breach (Fig. 29) revealed an intergranular fracture with no evidence of plastic deformation. The secondary breach (Fig. 30) had a similar crack morphology. The wall material adjacent to both breaching cracks was relatively fine grained. Wall sections on both sides of the main breach had an average of 17 grains/thickness, and sections adjacent to the secondary breach averaged 18 grains/thickness. Because capsule SRP-444 breached extensively, no sharp bends were visible on the transverse cross sections.

Although a minor amount of grain coarsening was observed on the interior of the shield cup (Fig. 31), the

cup microstructure was generally fine grained (Fig. 32). Slight grain coarsening was also observed on the vent cup interior (Fig. 33).

C. Vent Metallography

The capsule vents were carefully examined to determine the effects of the preimpact heat treatment (30 days at 1310°C) and to further define the impact response of the vent structure. Macroscopic examination revealed that both vents survived impact with only minor deformation (Figs. 34 and 35). No mechanical defects were observed in either vent, and both vent frits were uniform and properly aligned. A small crack was, however, observed in the SRP-423 vent assembly weld (Fig. 36). The crack was generally intergranular (Fig. 37) but did split a small grain near the inner surface. In addition, unusual amounts of grain growth were observed in wall sections adjacent to the vent cover welds in both capsules (Figs. 38 and 39).

Although significant amounts of fuel impurities were not detected in either vent, microscopic fuel fragments and small amounts of glassy oxides were entrapped in both frits. There was no evidence that the pretest heat treatment or subsequent impact had permitted the transport/deposition of fuel components to the capsule vents.

VII. FUEL CERAMOGRAPHY

Radiographic examination indicated that both fuel pellets were severely cracked before testing (Figs. 1 and 2); although it is not apparent in the radiographs, pellet HF-444 was reported to be nonintegral at loading (two pieces). Postimpact examination of the as-opened fuel capsules (Figs. 40 and 41) revealed that both pellets were badly fragmented. The fuel in capsule SRP-444 fractured cleanly along an axial plane (Fig. 41) and pushed through the clad in a line running the length of the impact face (Fig. 8). Pellet HF-423 fractured in a more random manner (Fig. 40) and produced less clad damage.

After macroscopic examination, ceramographic specimens were obtained from the center and exterior of each fuel pellet. The fuel microstructures are seen in Figs. 42-45. The micrographs show slight differences between fuel pellets and from point to point within each pellet. The small microstructural variations that were observed would not be expected to affect the overall impact response.

VIII. CHEMICAL ANALYSES

A. Iridium Alloy Chemistry

Samples for chemical analysis were removed from each of the iridium cups and were submitted for spectrographic and Auger electron spectroscopic examination. Spectrographic analysis was used to determine the bulk composition of each specimen, and Auger electron spectroscopy was used to determine the distribution of various elements on a fresh fracture surface. Results of the analyses are presented in Tables IX and X.

The spectrographic analyses (Table IX) indicate that the iridium alloy was reasonably consistent; there was little cup-to-cup variation in chemistry. The slight differences that were observed would not be expected to have any effect on the impact response. The DIT-5 cup chemical impurity levels were similar to those of cups used in previous Design Iteration Tests.

The results of the Auger analyses (Table X) indicate that high concentrations of carbon, oxygen, and sulfur were present in the iridium grain boundaries. Although these elements may have an effect on mechanical behavior, there were no indications of excessive grain growth or other abnormalities in the Auger specimens.

B. Fuel Chemistry

Samples for chemical analysis were removed from each of the DIT-5 fuel pellets. The results of spectrographic analyses, as well as the results of wet chemistry and radioanalysis for phosphorus, are presented in Table XI. The results indicate that the DIT-5 fuel pellets were chemically similar to one another and to the fuel pellets used in previous tests. Although the calcium and tantalum contents were abnormally high, neither ele-

ment would be expected to have affected the impact response of the fuel pellet or the clad.

IX. RELEASE DATA

To estimate the fuel release, the DIT-5 aeroshell and impact shell were radioanalyzed for plutonium. The results indicated that the aeroshell contained ~0.025 g of Pu, while the GIS held 0.329 g. Combining the values gives a total Pu weight of 0.354 g, the amount of plutonium present in 0.402 g of $^{238}\text{PuO}_2$ fuel.

X. DISCUSSION

DIT-5 was designed to provide data on the relative strengths of closure welds made with two- and four-pole arc oscillators. In this regard the test failed. Impact orientation, fuel breakup, and extensive wall failure prevented the development of significant loads across the capsule welds. Although both capsules breached, the cracks were transverse to the weld centerlines and unrelated to the welding procedures.

Both capsule failures apparently resulted from the differential displacement of large fuel fragments. The SRP-444 fuel pellet fractured along an axial plane (Fig. 41) and pushed through the clad in a line running the length of the impact face (Fig. 8). Because the SRP-423 pellet fractured in a more random manner (Fig. 40), the clad damage was less extensive (Fig. 7). Clad failure apparently becomes probable whenever the fuel breakup and external capsule support permit large fuel fragments to move across one another. The iridium is in effect only a membrane and cannot prevent the displacement of large fuel fragments or follow the resulting contours. Capsule survivability appears to improve

TABLE IX. Spectrographic Analyses of the Iridium-Alloy Cups Used in DIT-5^a

(All results are given in ppm by weight)

Element	SRP-423		SRP-444	
	Vent Cup	Shield Cup	Vent Cup	Shield Cup
Al	50	50	50	50
Cr	<10	<10	10	10
Cu	20	15	3	15
Fe	80	70	100	80
Ni	60	70	60	50
Si	10	20	<10	<10
W ^b				

^aElements are listed only if they exceed detectability limits in at least one cup.

^bAll cups had tungsten content of between 10^3 and 10^4 ppm.

TABLE X. Auger Intensity Ratios of DIT-5 Samples

Capsule	Cup	Location	Th ₄₅ /Ir ₂₂₉	C ₂₇₀ /Ir ₂₂₉	O ₅₁₀ /Ir ₂₂₉	S ₁₅₀ /Ir ₂₂₉
SRP-423	Vent	Inside	0.440	0.100	0.960	0.089
		Center	0.485	0.061	1.212	0.121
		Outside	0.609	0.174	1.696	0.696
	Blind	Inside	0.408	0.061	0.959	0.571
		Center	0.511	0.064	1.234	0.213
		Outside	0.531	0.143	1.143	0.571
SRP-444	Vent	Inside	0.526	0.158	1.263	---
		Center	0.500	0.100	1.050	---
		Outside	0.625	0.313	1.250	---
	Blind	Inside	0.432	0.163	0.674	0.081
		Center	0.651	0.256	0.744	---
		Outside	0.512	0.418	0.860	0.116

when the amount of external capsule support is increased or when the fuel is modified such that breakup into large fragments is unlikely. This conclusion assumes that fuel used in the DIT test series is representative of the at-launch condition. The possibility exists

that factors such as vibration testing, transport, and final loading would significantly alter the fuel response.

Metallographic examination of the clad failures did not reveal any unexpected features. All of the breaching cracks had a brittle, intergranular appearance (Figs. 22, 29, and 30). Although the breach in capsule SRP-444 intersected the weld, there was no evidence of direct weld involvement. The ductility of wall material in a reverse bend only 4 mm from the SRP-423 breach (Fig. 23) illustrates the importance of strain state in determining the failure of DOP-26 iridium.

Examination of the DIT-5 closure welds revealed that the SRP-444 (four-pole) weld had a somewhat more refined microstructure than the SRP-423 (two-pole) weld had. Sections of both welds contained significant porosity (Figs. 13 and 18). Although the SRP-444 closure weld contained a segment of incomplete weld penetration (Fig. 20), there was no indication that this defect had affected the capsule response. Numerous small cracks were observed on the interior surfaces of both closure welds (Figs. 10 and 15). All of the cracks were intergranular (Figs. 11 and 16) and apparently resulted from the severe capsule deformations. Two small cracks observed near the SRP-423 weld submergence (Fig. 9) were located in a section that experienced little deformation; the cracks probably predated the impact.

The void observed in a transverse section of the SRP-423 vent cup (Fig. 25) is interesting because of its size and location. The void was nearly 3 mm above the weld centerline and had a diameter equivalent to 25% of the total wall thickness. Although a similar defect was observed in a DIT-4 capsule weld,⁴ the SRP-423 void was outside the fusion zone and probably near the border of the heat-affected zone.

TABLE XI. Chemical Analyses of the DIT-5 Fuel Pellets^a

(All results are given in ppm by weight)

Element	SRP-423	SRP-444
Ag	10	5
Cr	20	35
Mo	3	3
Ta	250	250
Al	40	50
Ca	40	500
Na	8	40
Ti	80	100
B	3	5
Fe	55	140
Si	15	35
Ba	3	<2
Mn	1	3
Pb	10	<5
Ni	<5	6
P ^b	5	4
P ^c	<20	<20

^aElements are listed only if they exceed detectability limits in at least one pellet.

^bPhosphorus content determined by wet chemistry.

^cPhosphorus content determined by radioanalysis.

The iridium cup microstructures were generally fine grained and contained few defects. The cup grain sizes ranged from 15 to 22 grains/thickness. The results of microhardness tests (presented in Table VII) indicated that the cup hardnesses were acceptable and well within the range established by previous test clads. Both capsules contained isolated areas of abnormal grain growth in wall sections adjacent to the vent cover welds (Figs. 38 and 39). The occurrence of such localized grain growth at the same location in two relatively fine-grained capsules suggests that the grain coarsening is possibly related to some aspect of the cup production process. Chemical analyses of the iridium cups and $^{238}\text{PuO}_2$ fuel pellets did not reveal any abnormalities that could be correlated with the grain growth.

Spectrographic and Auger electron spectroscopic analyses (Tables IX and X) indicate that the iridium alloy was consistently of good quality. The cups in both capsules had similar chemical analyses; all variations were within the ranges established by the analyses of previous test clads. Although the Auger results indicated the presence of sulfur and oxygen in the iridium grain boundaries, there was no evidence that either element had affected the impact responses. There also was no evidence of thorium depletion in either capsule.

The DIT-5 fuel pellets were chemically and microstructurally similar to one another and to the fuel pellets used in previous DIT tests. The postimpact appearance of the fuel pellets and results of the SRP-423 sieve analysis (Tables V and VI) indicate that the mechanical responses of these fuel pellets were qualitatively similar to those of pellets tested in DIT-1, DIT-2, DIT-3, and DIT-4.

XI. CONCLUSIONS

1. DIT-5 was designed to provide data on the relative strengths of closure welds made with two- and four-pole arc oscillators. This objective was not met; module orientation, fuel breakup, and extensive clad failure prevented the development of significant loads across the capsule welds.

2. The extensive clad failures apparently resulted from the differential displacement and subsequent push-through of large fuel fragments. The iridium clad is a thin membrane; ductility is dependent on strain state and is not sufficient to follow the sharp contours produced by differential displacement of large fuel fragments.

3. The capsule welds were of questionable quality; porous sections were observed in both welds. Incomplete penetration occurred over a 120° arc of the four-pole closure weld.

4. Metallographic examination revealed that the microstructure of the four-pole weld was more refined and presumably stronger than that of the two-pole weld.

5. Unusual and potentially dangerous grain coarsening occurred in wall sections adjacent to the vent cover welds. Such localized grain growth at the same location in two relatively fine-grained capsules suggests a relation to some aspect of the cup production process.

6. Although the total fuel release is unknown, approximately 0.402 g of $^{238}\text{PuO}_2$ were trapped within the GIS and aeroshell.

7. The microstructures and chemical analyses of the fuel pellets and iridium alloy cups indicate that these components were similar to those tested in DIT-1, DIT-2, DIT-3, and DIT-4. Because no structural or chemical anomalies that could have affected the impact response were observed, the behavior of the DIT-5 test components should be considered typical.

8. The mechanical performance of the vents in both DIT-5 capsules was satisfactory; no defects were observed in either vent.

ACKNOWLEDGMENTS

We wish to thank J. Archuleta, L. Bergamo, and D. Pavone for their generous laboratory assistance.

REFERENCES

1. F. W. Schonfeld, "General-Purpose Heat Source Development: Safety Test Program, Postimpact Evaluation, Design Iteration Test 1," Los Alamos National Laboratory report LA-9680-SR (April 1984).
2. F. W. Schonfeld and T. G. George, "General-Purpose Heat Source Development: Safety Test Program, Postimpact Evaluation, Design Iteration Test 3," Los Alamos National Laboratory report LA-10034-SR (July 1984).
3. F. W. Schonfeld and T. G. George, "General-Purpose Heat Source Development: Safety Test Program, Postimpact Evaluation, Design Iteration Test 2," Los Alamos National Laboratory report LA-10012-SR (June 1984).
4. T. G. George and F. W. Schonfeld, "General-Purpose Heat Source Development: Safety Test Program, Postimpact Evaluation, Design Iteration Test 4," Los Alamos National Laboratory report LA-10217-SR (December 1984).
5. "Iridium Weld Inspection Data Sheet (Metallography Lab)," E. I. duPont de Nemours & Co., Savannah River Plant Operations Manual DPSOP-268 procedure DPSOL-235-F-PuFF-3129M, Rev. 1 (March 1981).

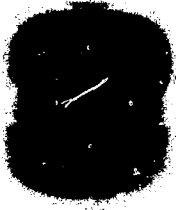


Fig. 1. Radiographic prints of the as-received fuel capsules. (a) SRP-444 and (b) SRP-423. Approximately 1X.

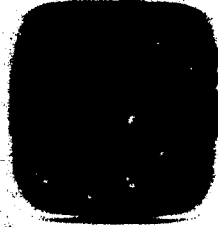


Fig. 2. Radiographic prints of the fuel capsules after aging at 1310°C for 30 days. (a) SRP-444 and (b) SRP-423. Approximately 1X.

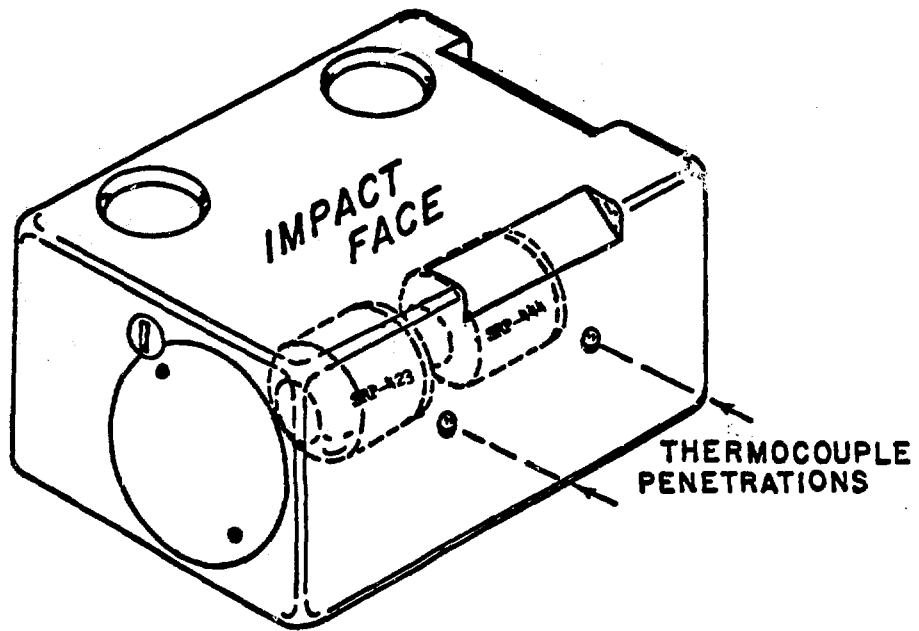


Fig. 3. Test diagram.

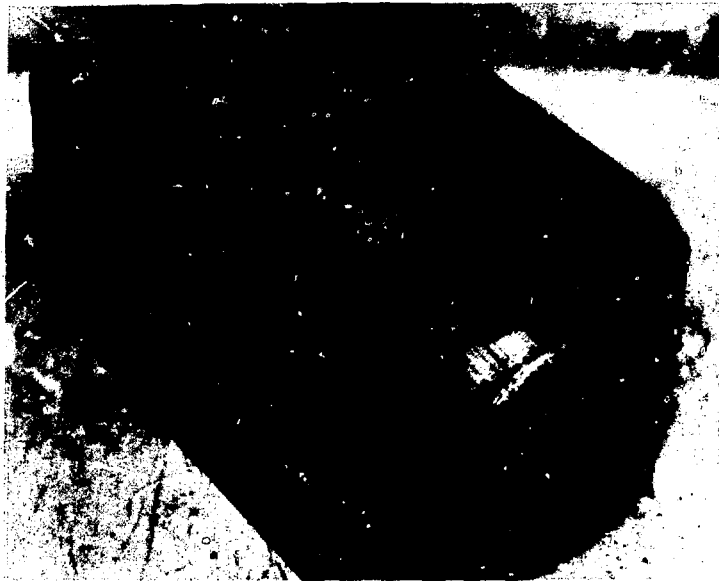
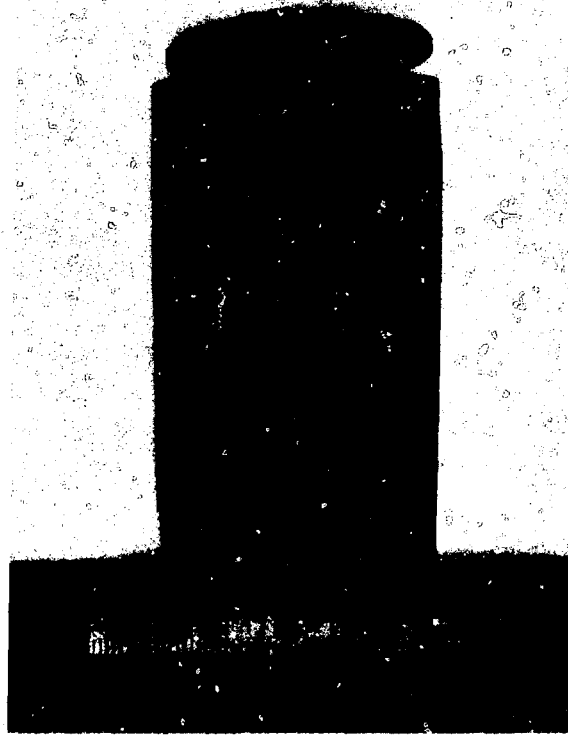
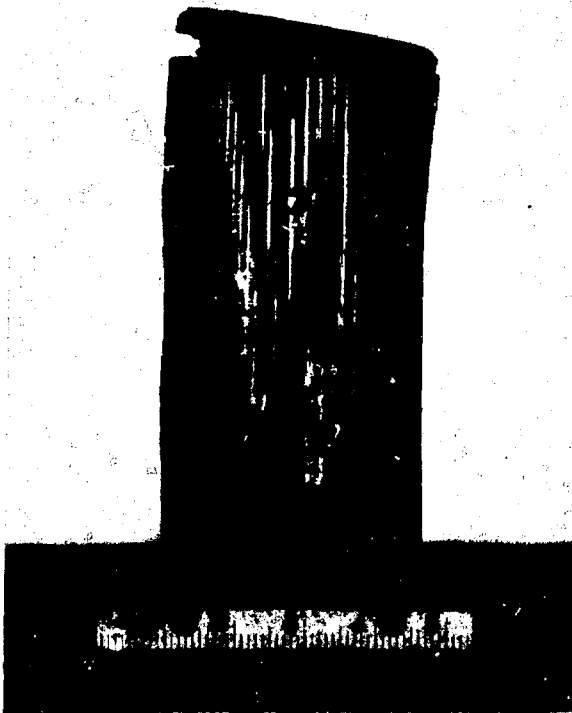


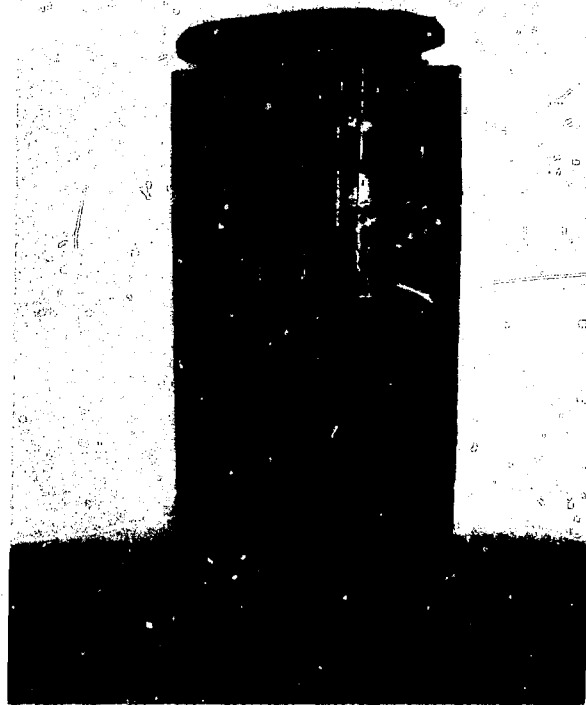
Fig. 4. The DIT-5 aeroshell and impact shell were damaged by the impact, but the fueled clads were not released. IX.



(a)



(b)



(c)

Fig. 5. The DIT-5 impact shell sustained a significant amount of damage. (a) Impact face, (b) profile, and (c) trailing face. All at 1X.

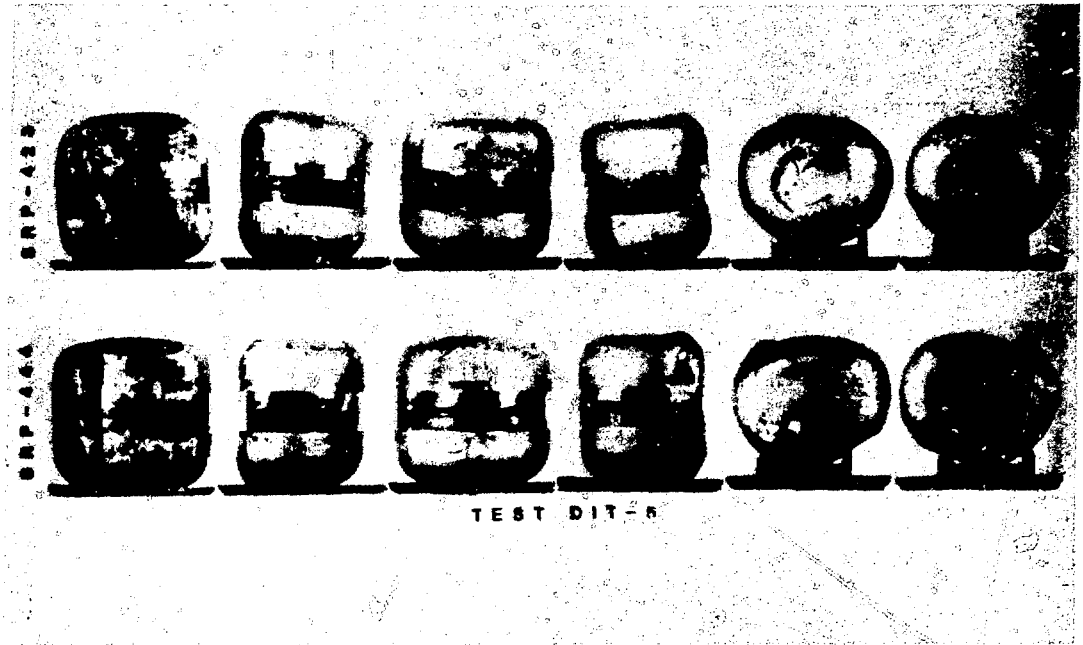
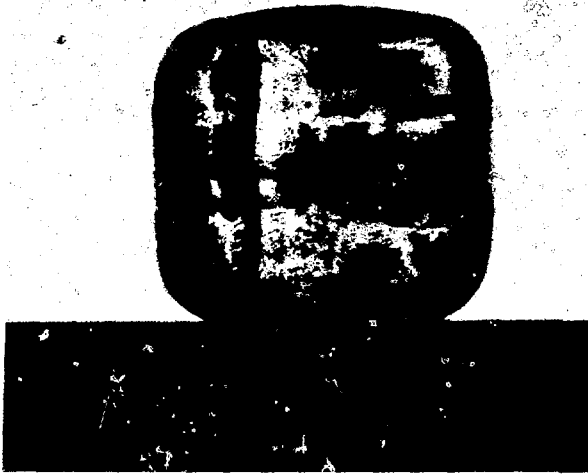


Fig. 6. The capsule deformations were consistent with the clad deformations observed in other flat-on impacts. 1X.



Fig. 7. Capsule SRP-423 was breached by a narrow crack on the impact face of the vent cup; the crack is at the left of the impact face. 1.5X.



(a)



(b)



(c)

Fig. 8. The impact face of capsule SRP-444 was divided by a wide crack that extended into the vent cup radii. (a) Impact face, (b) vent end, and (c) blind end. All at 1.5X.

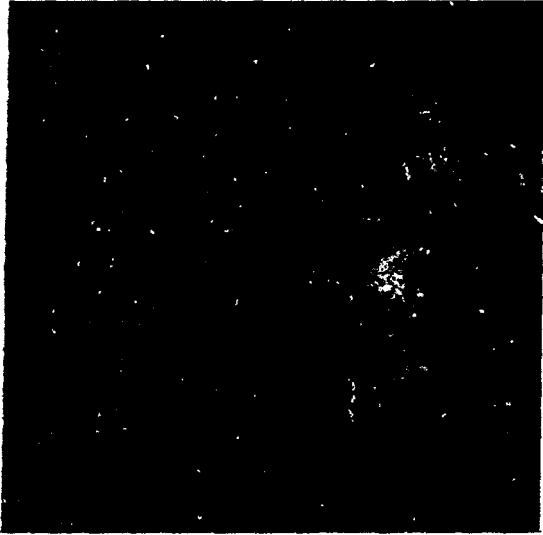
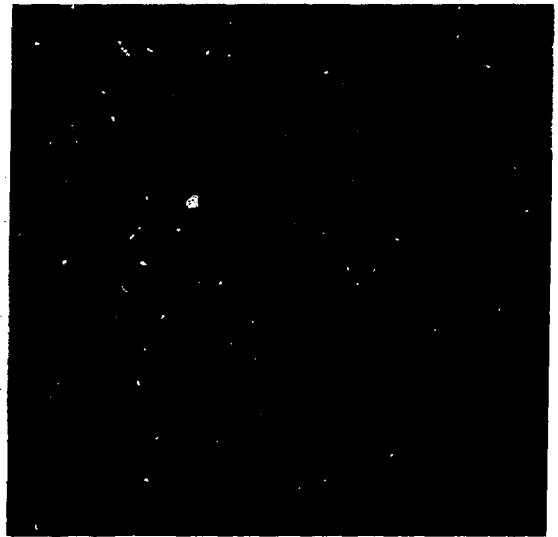
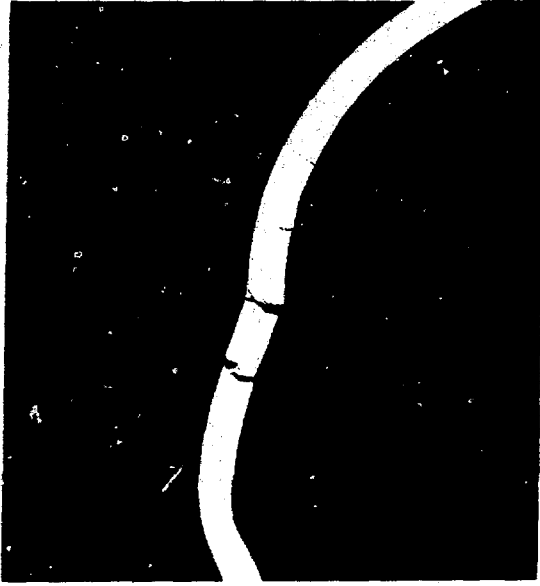


Fig. 9. Two small cracks were observed near the SRP-423 weld submergence. 10.0X.

Fig. 10. Deep weld cracks were visible in a reverse bend on the SRP-423 impact face. 10.0X.



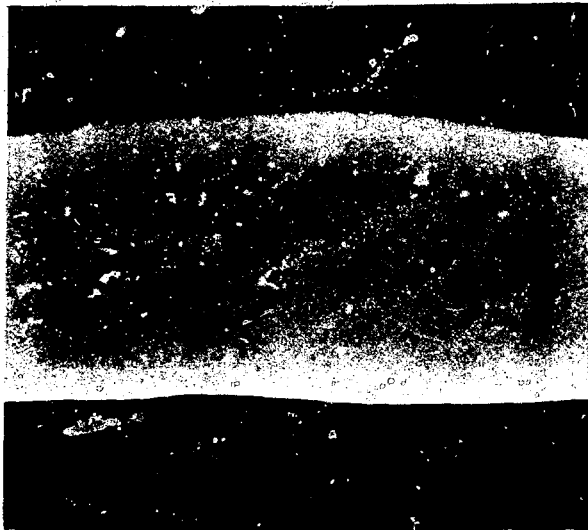


(a)

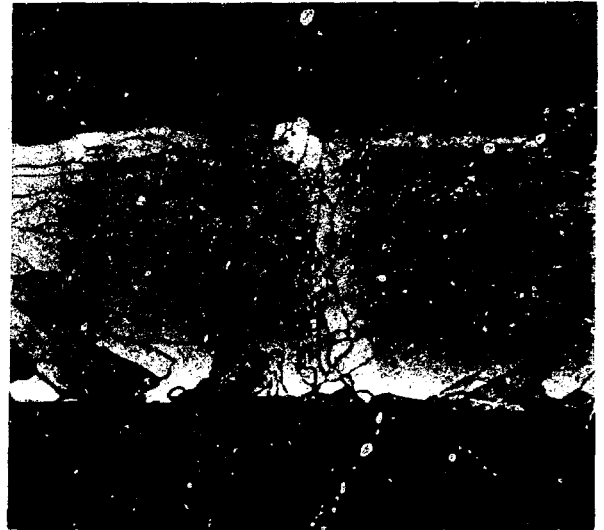


(b)

Fig. 11. Two cracks in the SRP-423 closure weld penetrated the capsule wall. (a) As polished, 7X, and (b) as etched, 50X.



(a)



(b)

Fig. 12. The SRP-423 single-pass weld was free of defects. (a) As polished and (b) as etched. Both at 50X.



(a)



(b)

Fig. 13. The SRP-423 overlap specimen contained a significant amount of porosity and had a coarse microstructure. (a) As polished and (b) as etched. Both at 50X.

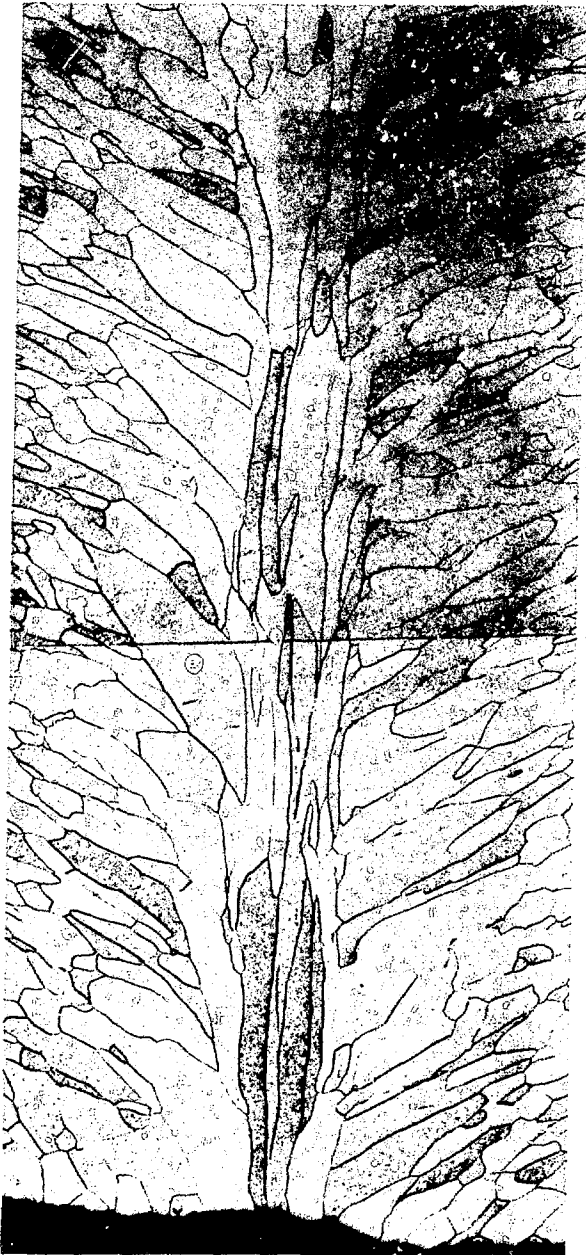


Fig. 14. The SRP-423 face-on weld microstructure was typical. 50X.

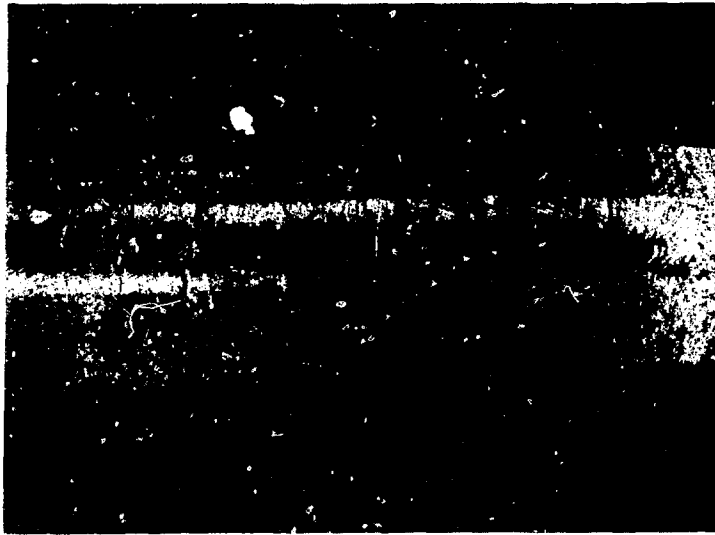
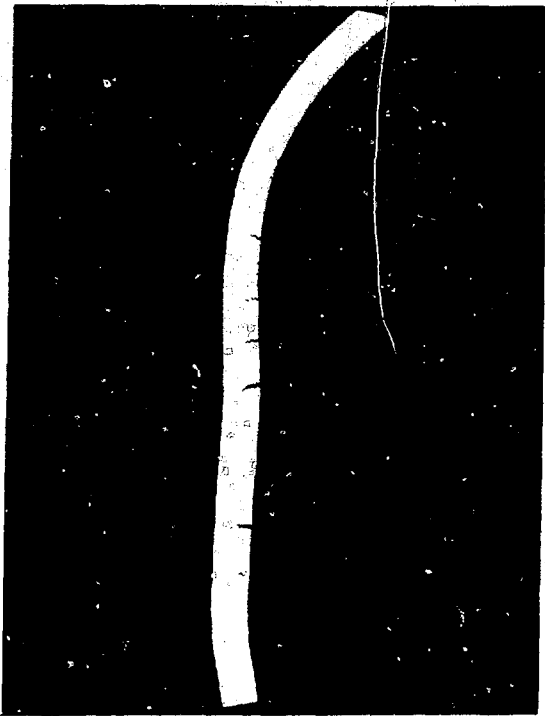


Fig. 15. Numerous transverse weld cracks were observed in a reverse bend on the SRP-444 impact face. 10X.



(a)

(b)



Fig. 16. Weld cracks on the SRP-444 impact face penetrated more than 50% of the wall thickness. (a) As polished, 7X, and (b) as etched, 50X.

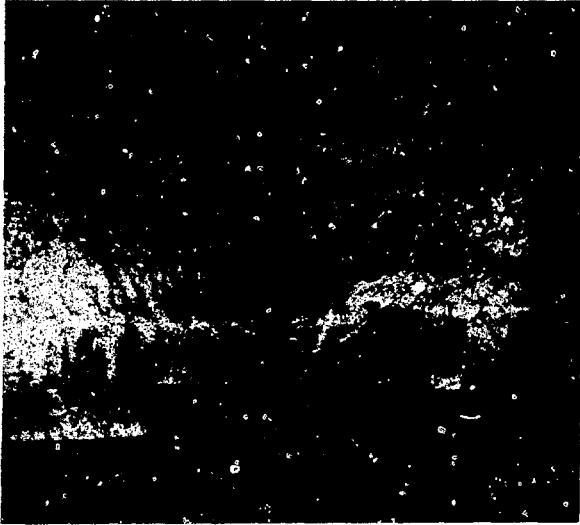


Fig. 17. The SRP-444 closure weld was free of defects at the point of weld submergence. 10X.



(a)



(b)

Fig. 18. The overlap region of the SRP-444 weld contained an unusual amount of porosity. (a) As polished and (b) as etched. Both at 50X.



Fig. 19. In sections of complete penetration, the SRP-444 closure weld had a typical single-pass microstructure. Etched, 50X.



Fig. 20. The SRP-444 single-pass microstructure was only slightly abnormal in the sections of incomplete weld penetration. Etched, 50X.

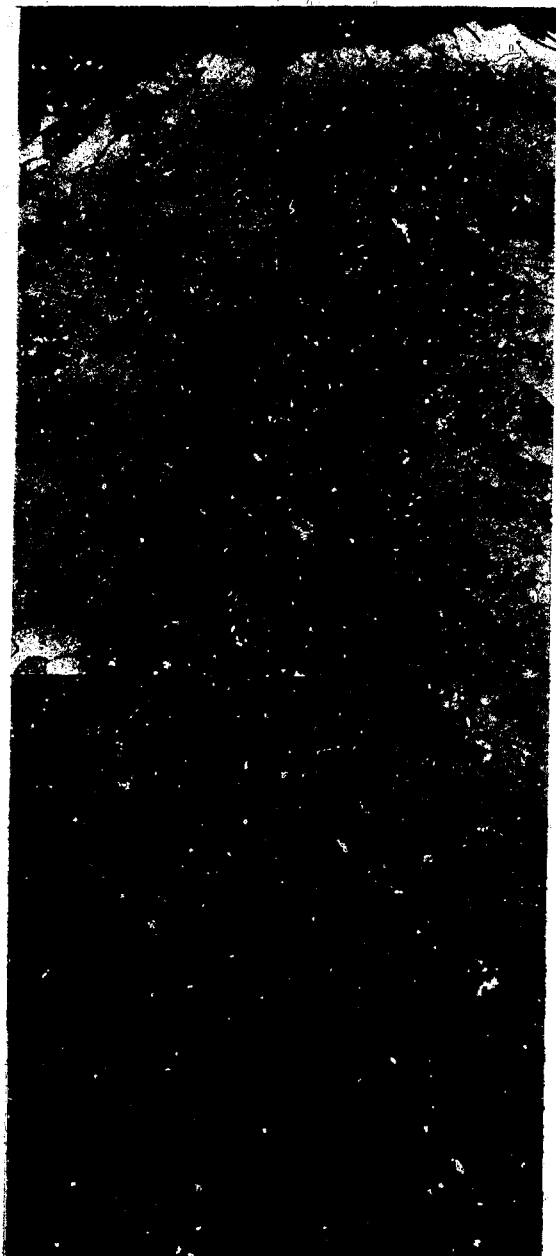
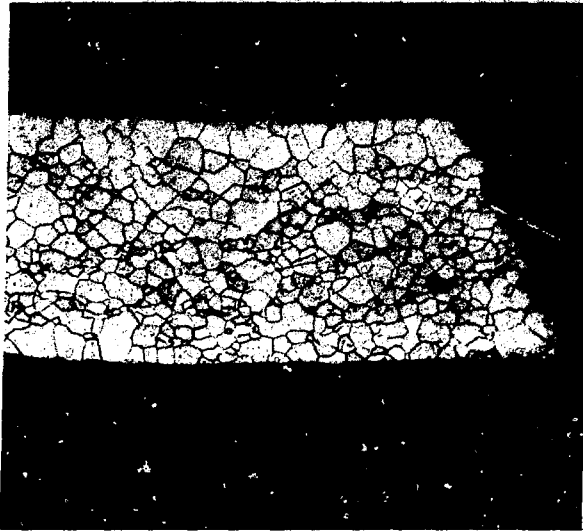
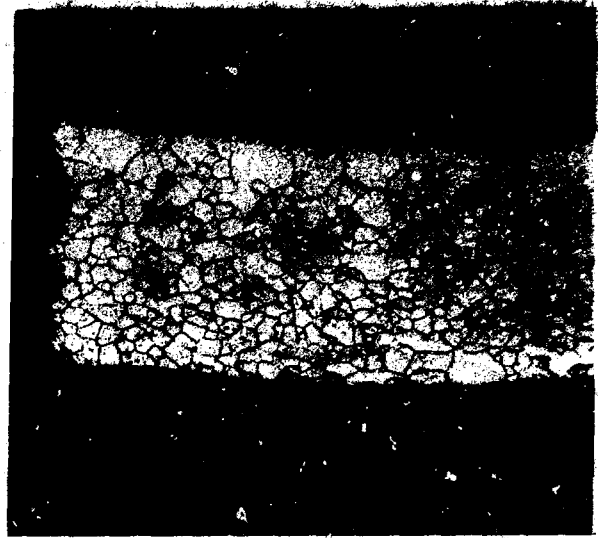


Fig. 21. The SRP-444 closure weld had a typical face-on microstructure. Etched, 50X.



(a)



(b)

Fig. 22. The breach in capsule SRP-423 displayed the same intergranular morphology observed in previous clad failures. (a) Left side of impact face and (b) right side. Both at 50X.

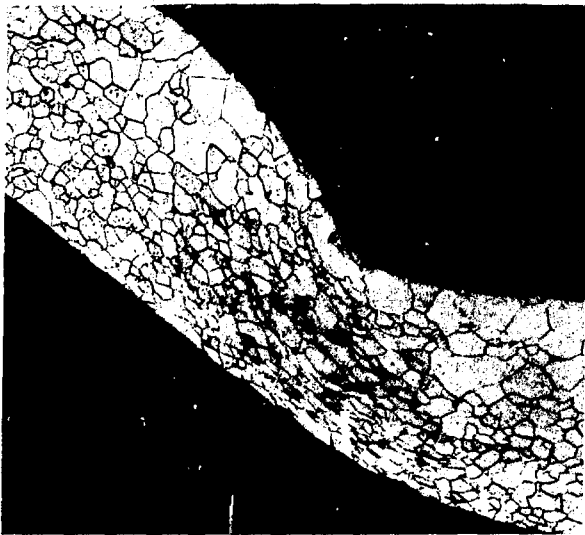


Fig. 23. A significant amount of grain elongation was observed in a reverse bend on the SRP-423 impact face. 50X.

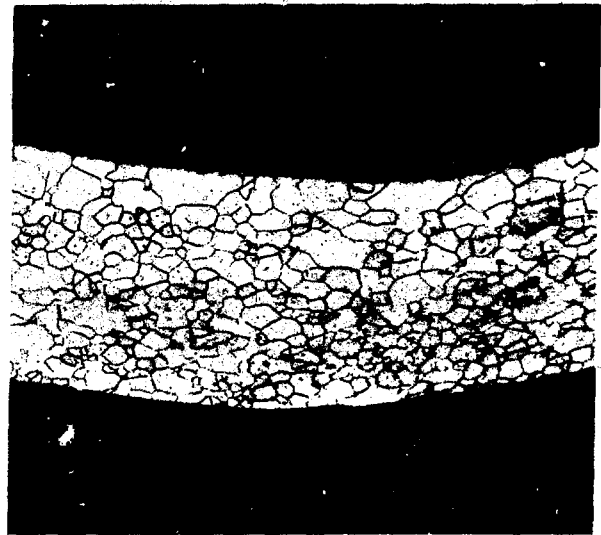


Fig. 24. There was no evidence of cracking in a sharp bend on the SRP-423 impact face. 50X.



Fig. 25. A large void was observed in a transverse section removed from the SRP-423 impact face. 50X.

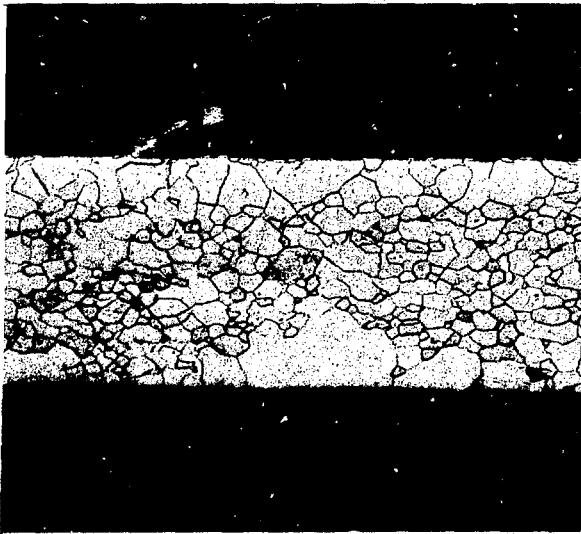
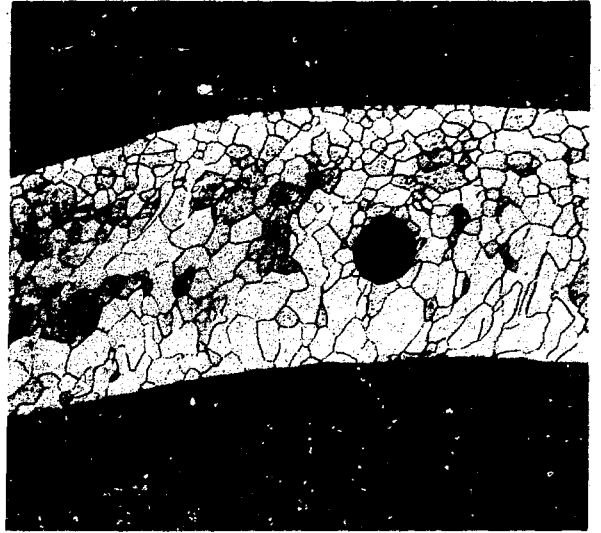


Fig. 26. Isolated areas of slight grain growth were observed in the SRP-423 vent cup. 50X.

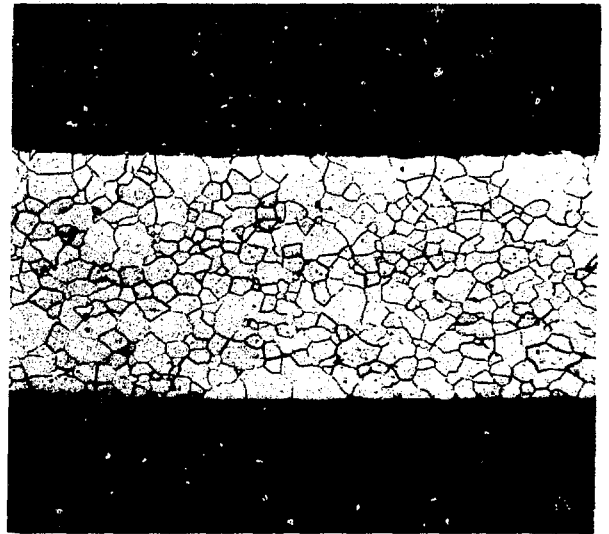


Fig. 27. The microstructure of the SRP-423 vent cup was generally fine grained. 50X.

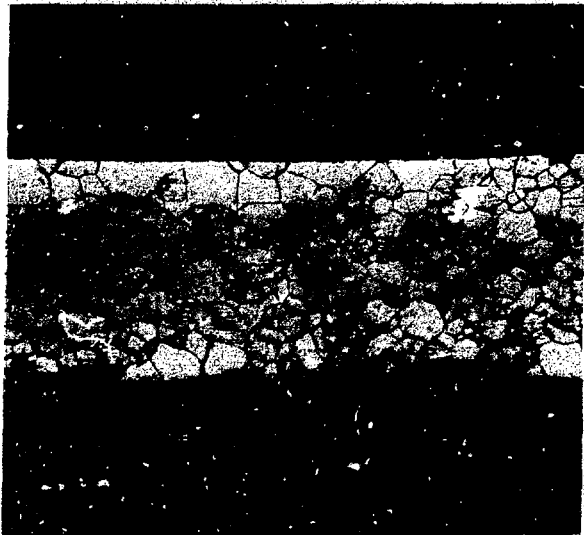
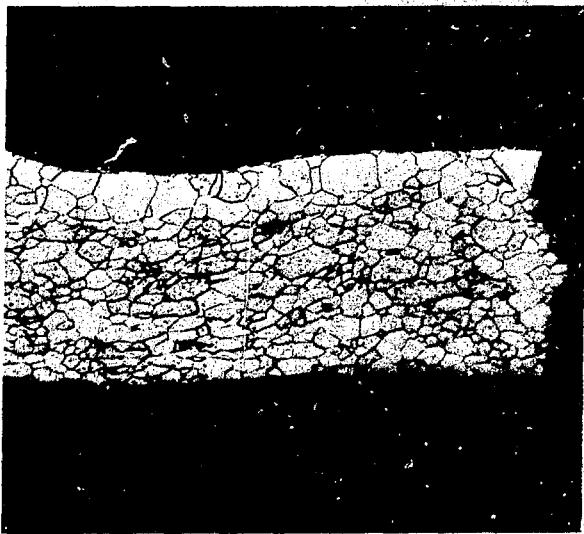
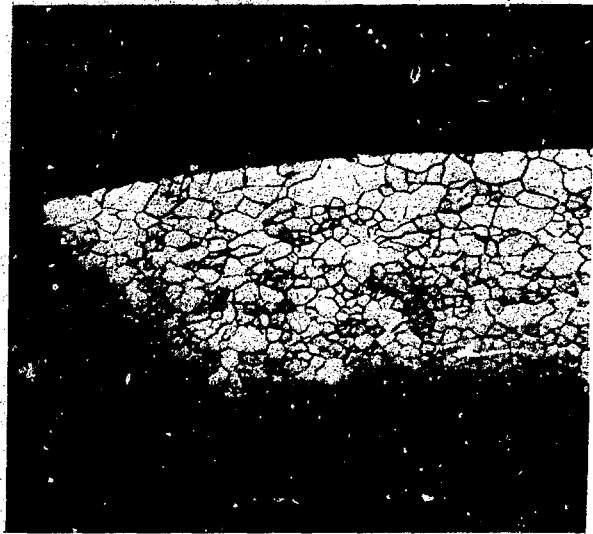


Fig. 28. The SRP-423 weld-shield cup had an average of 15.5 grains/thickness. 50X.

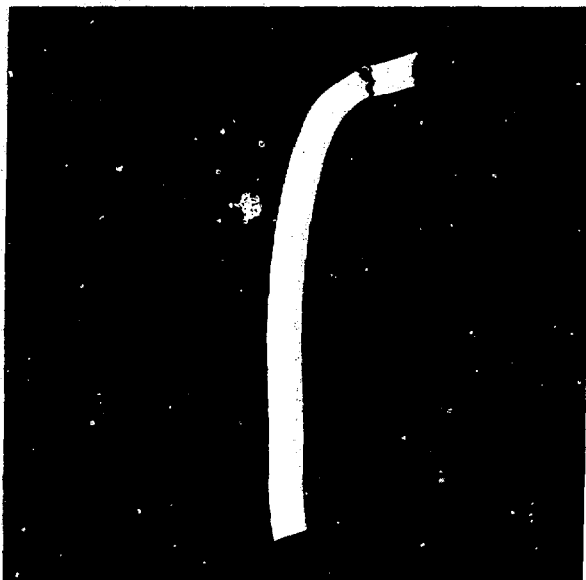


(a)



(b)

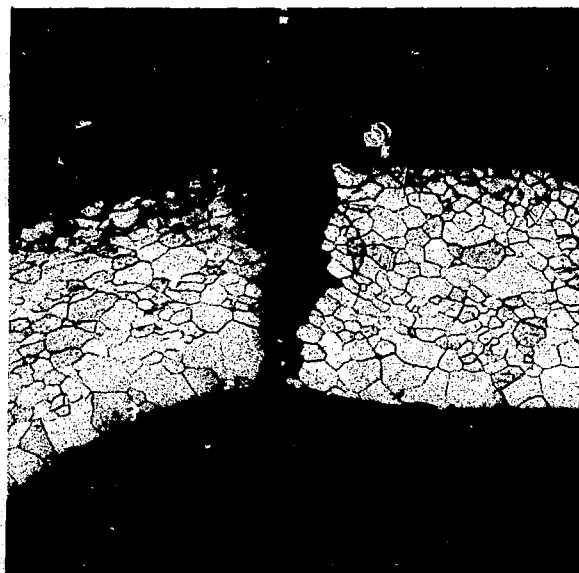
Fig. 29. The main breach in capsule SRP-444 was intergranular. (a) Left side of impact face and (b) right side. Both at 50X, etched, 50X.



(a)



(b)



(c)

Fig. 30. The secondary breach in SRP-444 also had a brittle, intergranular appearance. (a) As polished, 7X; (b) as polished, 50X; and (c) as etched, 50X.

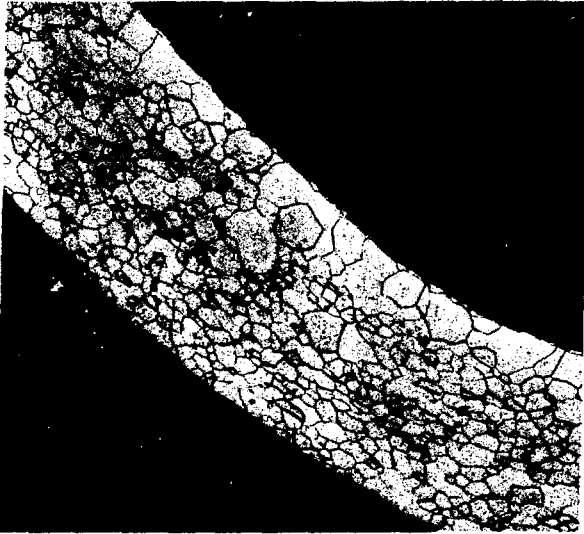


Fig. 31. A minor amount of grain coarsening was observed on the interior of the SRP-444 weld-shield cup. 50X.

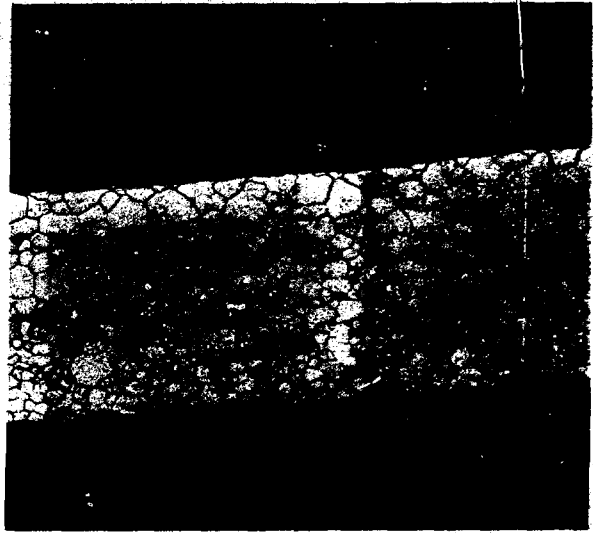


Fig. 32. The microstructure of the SRP-444 shield cup was generally fine grained. 50X.



Fig. 33. Slight grain coarsening was also observed on the interior of the SRP-423 vent cup. 50X.

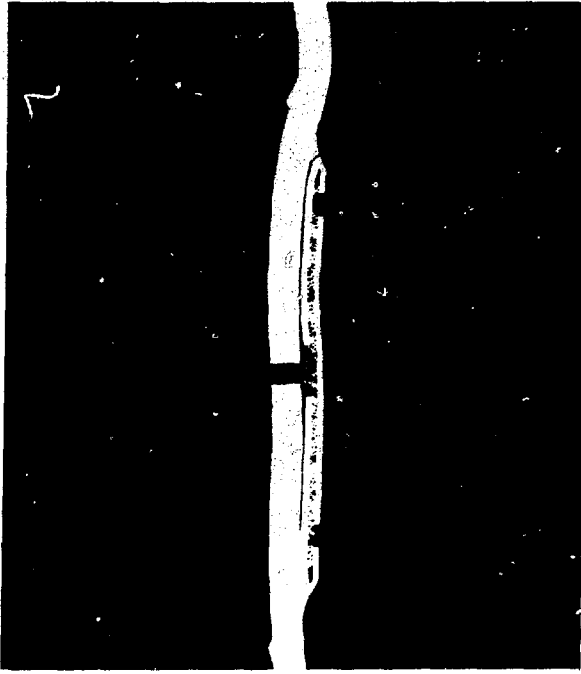


Fig. 34. The vent on capsule SRP-423 survived impact with only minor deformation. 7X.

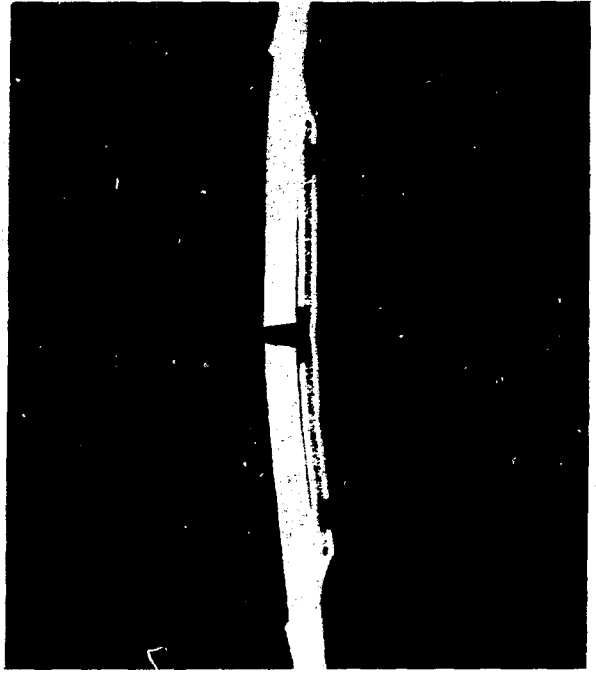


Fig. 35. The SRP-444 vent was undamaged. 7X.

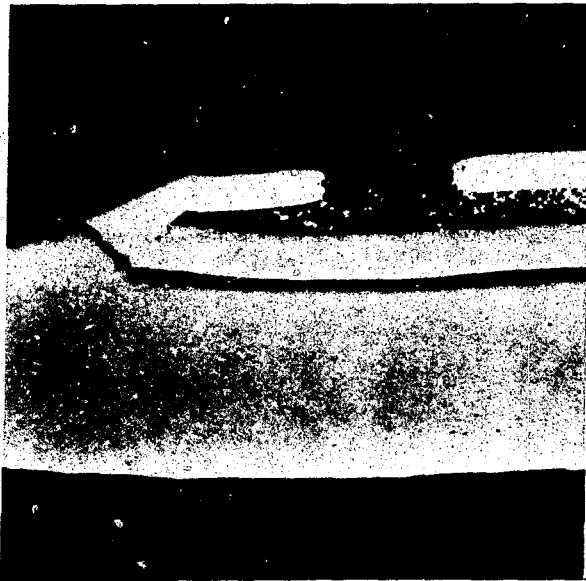


Fig. 36. A small crack was observed in the SRP-423 vent assembly weld. As polished, 40X.

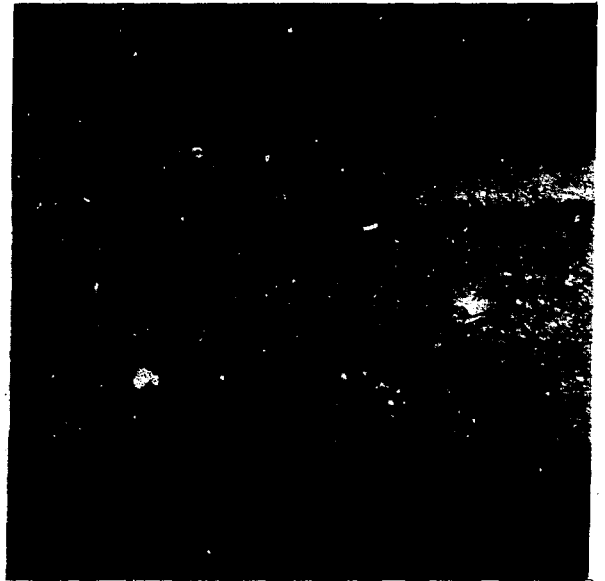
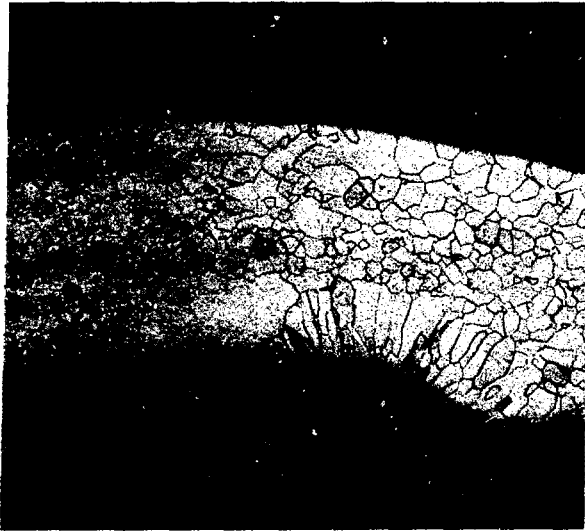
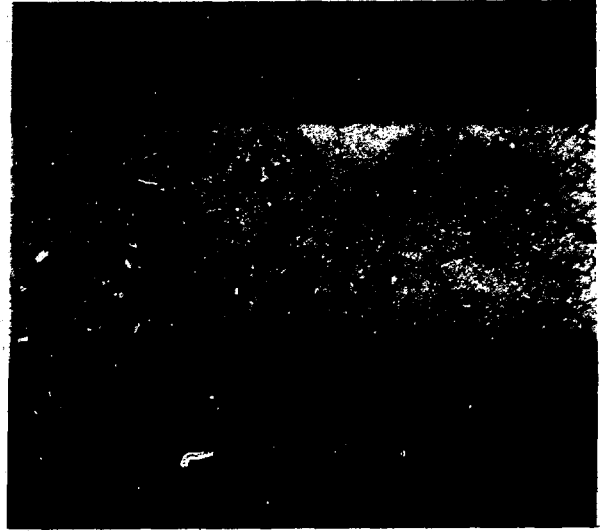


Fig. 37. The crack in the SRP-423 vent assembly weld was almost exclusively intergranular. Etched, 50X.

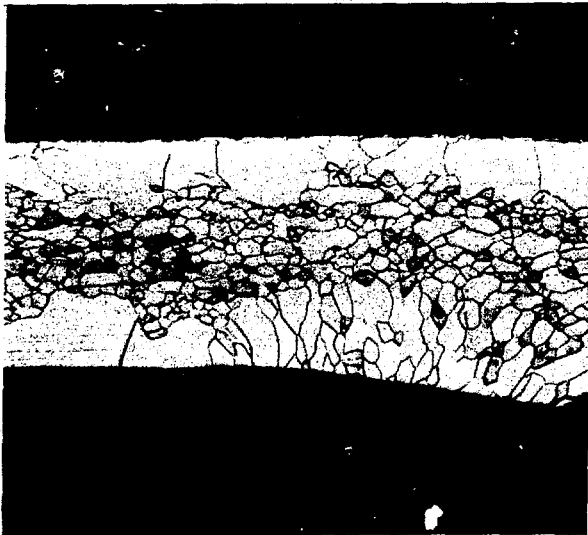


(a)

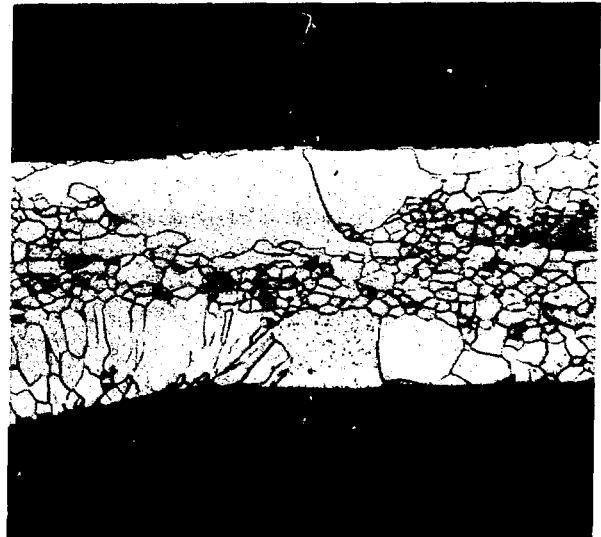


(b)

Fig. 38. Wall sections adjacent to the SRP-423 vent cover weld were unusually coarse grained. (a) Impact face side, and (b) opposite face. Both at 50X.



(a)



(b)

Fig. 39. Abnormal grain growth was also observed near the SRP-444 vent cover weld. (a) Impact face side and (b) opposite face. Both at 50X.

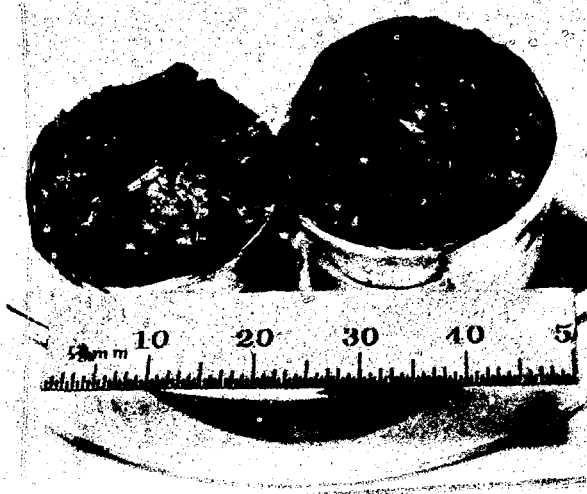
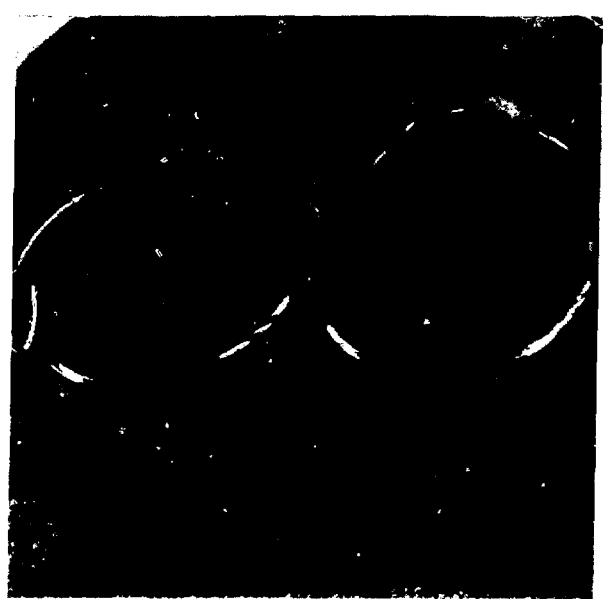


Fig. 40. The fuel in capsule SRP-423 fractured in a brittle manner. 1.5X.

Fig. 41. The SRP-444 fuel pellet fractured cleanly along an axial plane. 1.5X.

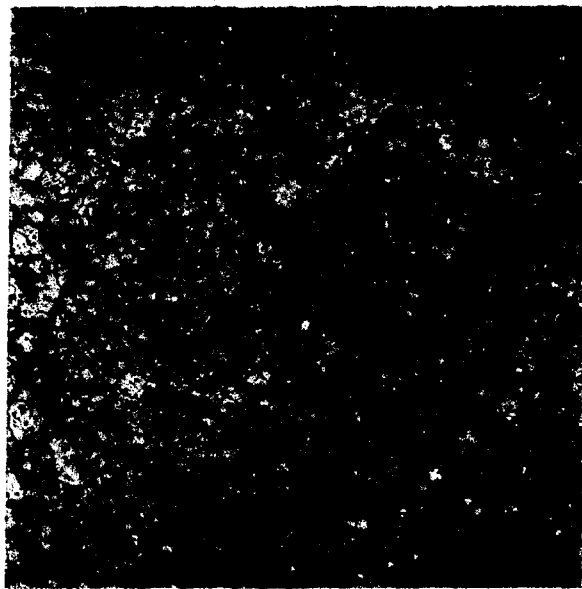




(a)

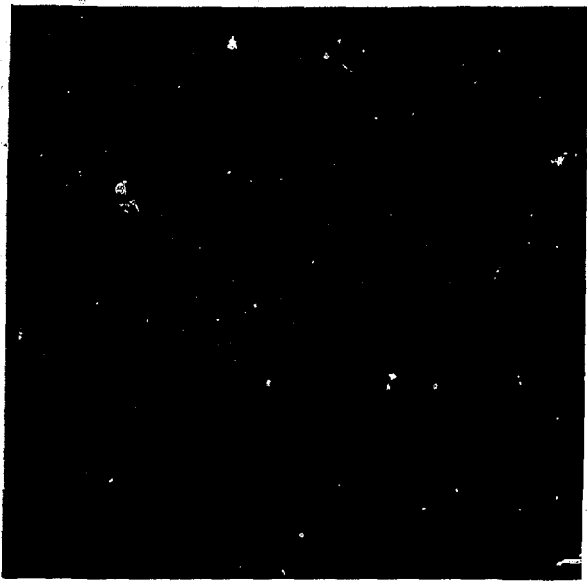


(b)

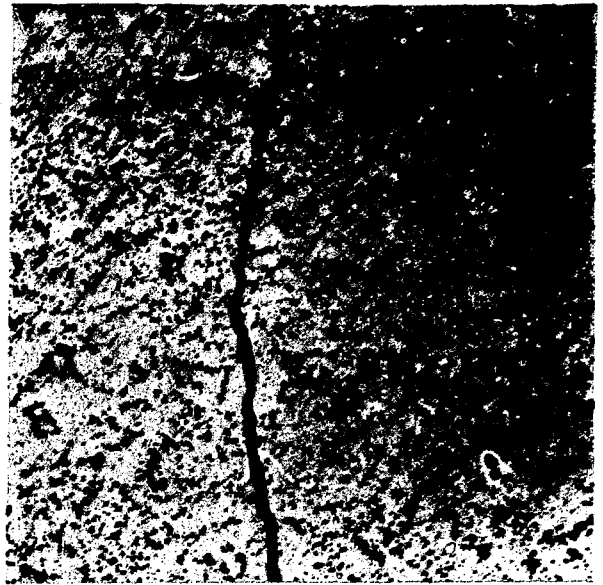


(c)

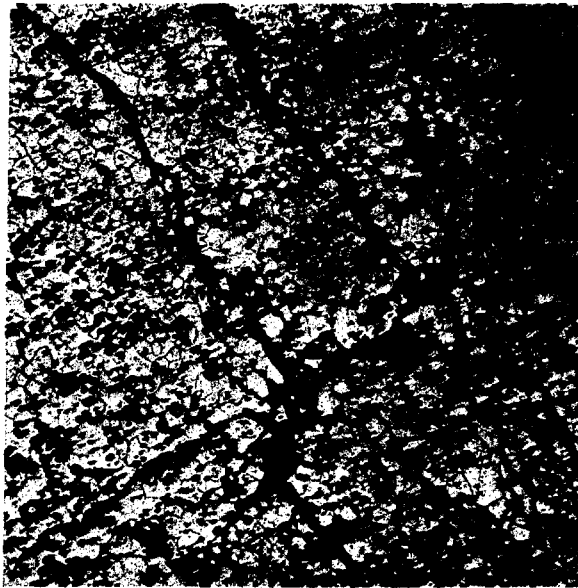
Fig. 42. Ceramographic specimen removed from the center of fuel pellet SRP-423. (a) Macrograph, 10X; (b) micrograph, as polished, 100X; and (c) as etched, 100X.



(a)

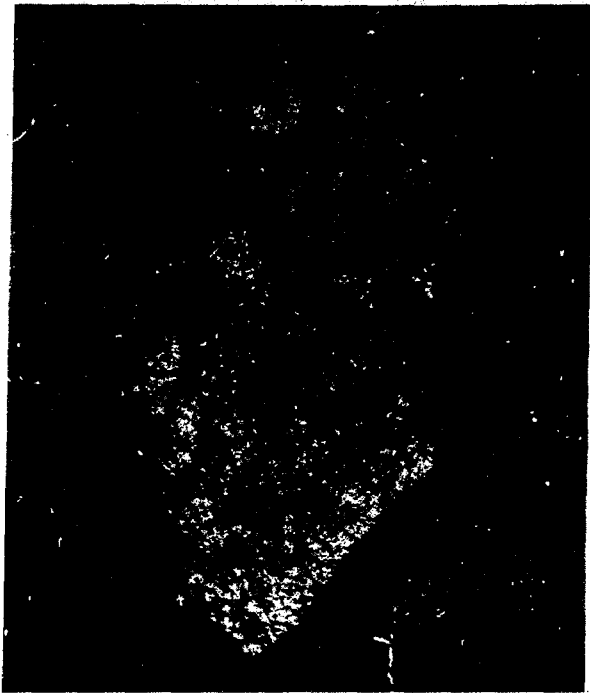


(b)

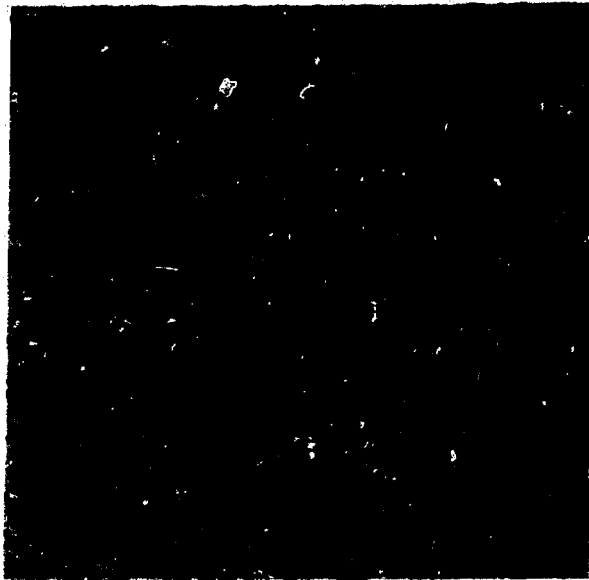


(c)

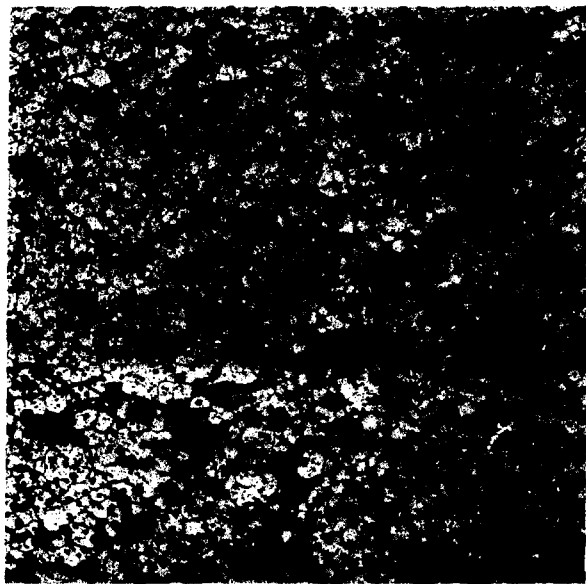
Fig. 43. Ceramographic specimen removed from the exterior of pellet SRP-423. (a) Macrograph, 10X; (b) micrograph, as polished, 100X; and (c) as etched, 100X.



(a)



(b)

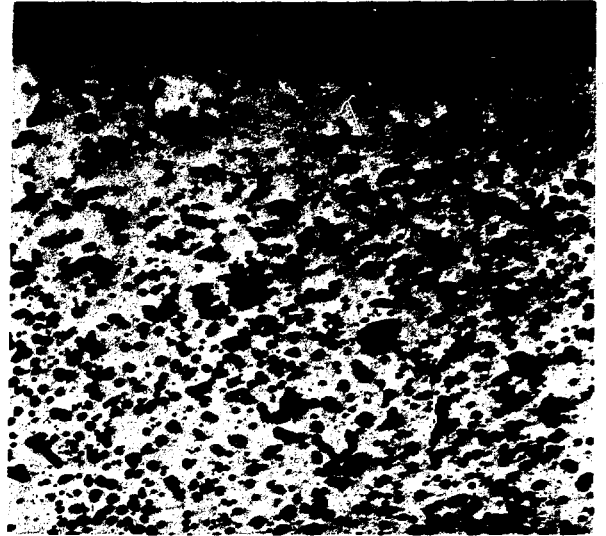


(c)

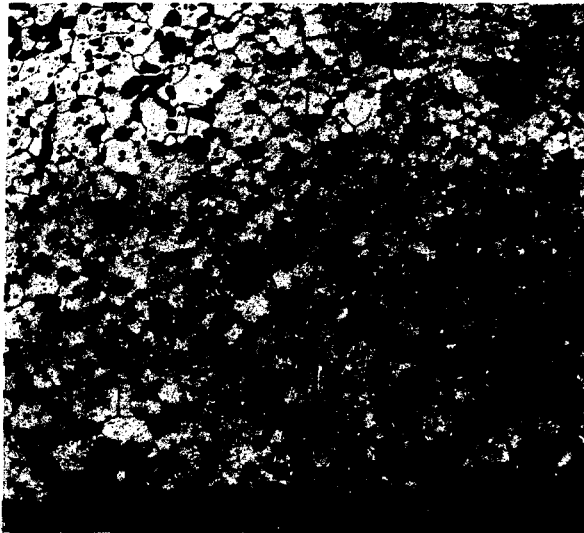
Fig. 44. Ceramographic specimen removed from the center of fuel pellet SRP-444. (a) Macrograph, 10X; (b) micrograph, as polished, 100X; and (c) as etched, 100X.



(a)



(b)



(c)

Fig. 45. Ceramographic specimen removed from the exterior of pellet SRP-444. (a) Macrograph, 10X; (b) micrograph, as polished, 100X; and (c) as etched, 100X.